RECLAMATION
Managing Water in the West

Desalination and Water Purification Research and Development Program Report No. 110

Impact of Magnetic Fields on Reverse Osmosis Separation: A Laboratory Study

University of South Florida

Agreement No. 01-FC-81-0739

U.S. Department of the Interior
Bureau of Reclamation

October 2005

REPORT DOCUMENTATION PAGE

Form Approved OMB No. 0704-0188

1. REPORT DATE *(DD-MM-YYYY)*
October 2005

2. REPORT TYPE
Final

3. DATES COVERED *(From - To)*

4. TITLE AND SUBTITLE
Impact of Magnetic Fields on Reverse Osmosis Separation: A Laboratory Study

5a. CONTRACT NUMBER
01-FC- 81-0739

5b. GRANT NUMBER

5c. PROGRAM ELEMENT NUMBER

6. AUTHOR(S)
Robert P. Carnahan, Ph.D., P.E.; Marilyn Barger, Ph.D., P.E.; Silvana Ghiu

5d. PROJECT NUMBER

5e. TASK NUMBER

5f. WORK UNIT NUMBER

7. PERFORMING ORGANIZATION NAME(S) AND ADDRESS(ES)
University of South Florida

8. PERFORMING ORGANIZATION REPORT NUMBER

9. SPONSORING / MONITORING AGENCY NAME(S) AND ADDRESS(ES)
U.S. Department of the Interior, Bureau of Reclamation,
Technical Service Center, Environmental Services Division,
Water Treatment Engineering and Research Group, D-8230,
PO Box 25007, Denver CO 80228

10. SPONSOR/MONITOR'S ACRONYM(S)

11. SPONSOR/MONITOR'S REPORT NUMBER(S)
Report No. 110

12. DISTRIBUTION / AVAILABILITY STATEMENT
Available from the National Technical Information Service (NTIS),
Operations Division, 5285 Port Royal Road, Springfield VA 22161

13. SUPPLEMENTARY NOTES

14. ABSTRACT ***(Maximum 200 words)***
This research investigated the effects of electromagnetic fields on salt and water transport in reverse osmosis (RO) membranes. Two experimental apparatus were considered—the PowerSurvivor-35 from PUR and a classic lab scale RO system. For both systems, the electromagnetic field was generated by a solenoid placed around the pressure vessel. The field intensity was 680 Gs, and the field frequency was 40 hertz (Hz) and 300 Hz. The studied salts were LiCl, NaCl, KCl, $MgCl_2$, and $CaCl_2$ at concentrations of 0.02 M, 0.05 M and 0.1 M. The preferential sorption-capillary flow model was used to calculate the transport parameters in the membrane.

15. SUBJECT TERMS
reverse osmosis, salt permeability, recovery rate, electromagnetic field, salt, field frequency, membrane transport parameters

16. SECURITY CLASSIFICATION OF: Nonsensitive			17. LIMITATION OF ABSTRACT	18. NUMBER OF PAGES	19a. NAME OF RESPONSIBLE PERSON
a. REPORT	b. ABSTRACT	c. THIS PAGE		33	Michelle Chapman
					19b. TELEPHONE NUMBER *(include area code)* 303-445-2264

Standard Form 298 (Rev. 8/98)
Prescribed by ANSI Std. 239-18

Desalination and Water Purification Research and Development Program Report No. 110

Impact of Magnetic Fields on Reverse Osmosis Separation: A Laboratory Study

University of South Florida

Agreement No. 01-FC-81-0739

U.S. Department of the Interior
Bureau of Reclamation
Technical Service Center
Environmental Resources Team
Water Treatment Engineering and Research Group
Denver, Colorado

October 2005

MISSION STATEMENTS

The mission of the Department of the Interior is to protect and provide access to our Nation's natural and cultural heritage and honor our trust responsibilities to Indian tribes and our commitments to island communities.

The mission of the Bureau of Reclamation is to manage, develop, and protect water and related resources in an environmentally and economically sound manner in the interest of the American public.

Disclaimer

Information contained in this report regarding commercial products or firms was supplied by those firms. It may not be used for advertising or promotional purposes and is not to be construed as an endorsement of any product or firm by the Bureau of Reclamation.

The information contained in this report was developed for the Bureau of Reclamation; no warranty as to the accuracy, usefulness, or completeness is expressed or implied.

Abstract

The objective of this research was to investigate the effects of electromagnetic fields on the salt and water transport in reverse osmosis membranes. Two experimental apparatus were considered—first, the PowerSurvivor-35 from PUR and second, a classic lab scale reverse osmosis (RO) system. For both systems, the electromagnetic field was generated by a solenoid placed around the pressure vessel. The field intensity was 680 Gs, and the field frequency was 40 hertz (Hz) and 300 Hz. The studied salts were LiCl, NaCl, KCl, $MgCl_2$, and $CaCl_2$ at concentrations of 0.02 M, 0.05 M and 0.1 M. The preferential sorption-capillary flow model was used to calculate the transport parameters in the membrane.

The PowerSurvivor-35 was inadequate for this research because the system operated at a constant recovery rate and the operating pressure could not be controlled. Moreover, the product temperature increased by about 3 degrees Celsius (°C) when the field was applied, and the effects of the field on the membrane transport parameters could not be separated from the temperature effects. Last, high temperatures developed in the solenoid determined the appearance of cracks in the pressure vessel.

The classic lab scale RO system was equipped with a cooling system placed between the solenoid and the pressure vessel. The product temperature increased by less than 1 °C when the electromagnetic field was applied. The system sustained long exposures to the field very well.

No effects of the electromagnetic field were observed on the pure water permeability, A. However, the continuous increase of A for more than 500 hours suggested that perhaps the membrane hydraulic properties were modified by the electromagnetic field. The salt permeability increased in the tests with no field and decreased for the tests when the electromagnetic field was applied. However, the differences in the average salt permeability with and without field are about 7 percent and are within the experimental errors. No differences in the salt permeability were observed when the frequency of the electromagnetic field was varied from 40 Hz to 300 Hz.

Table of Contents

List of Tables

List of Tables (continued)

List of Figures

1. Introduction

The interest in using reverse osmosis (RO) for seawater desalination has continuously increased in the last decade. Membrane scaling and fouling represent the major factors limiting the operation of RO desalination plants. Due to scaling and fouling, higher expenses were associated with membrane cleaning and membrane replacement. The use of cleaning solutions, antiscalants, or turbulence promoters to reduce the scaling/fouling potential is either costly or it has not yet been implemented.

This research investigates the impact of electromagnetic fields on the transport parameters in RO membranes. It is anticipated that the electromagnetic fields have an effect on the potential of scale formation by reducing the rate of salts transported through the membranes and by possibly modifying the hydraulic properties of the membrane quantified by the pure water permeability.

2. Objectives of the Project

The objectives of this research are as follows:

- To study the effects of electromagnetic fields on pure water permeation
- To study the effects of electromagnetic fields on the salt permeability
- To analyze the differences in the effect of electromagnetic fields on monovalent and divalent cations for salts with common anion
- To investigate the effect of the electromagnetic field frequency on both pure water and salt permeability

3. Methodology

Two experimental apparatus were used in this research. First, the watermaker PowerSurvivor-35 provided by PUR and referred as "Survivor unit" and second, a classic lab scale RO system, referred as "modified RO system" and described in section 7, "Appendix."

Survivor unit consisted of a positive displacement high pressure pump, a pressure vessel of 2 inches x 14 inches, and used a spiral wound RO membrane. The permeate flowrate was fixed at 5 liters per hour (L/h) and a fixed recovery rate of 9.3 percent. All feed solutions were contained in a 200-L tank with both the concentrate and the permeate recirculated back to this tank. A heat exchanger was used to maintain a constant temperature of 25 degrees Celsius (°C). Digital flow meters, conductivity, temperature and pH probes were used to measure the water quality of the feed and of the permeate. The data was monitored and collected in real time using a personal computer.

An electromagnetic (ELMG) field oriented parallel to the pressure vessel and perpendicular to the direction of water permeation was generated by a solenoid. The magnetic field strength was controlled by a current source. The intensity of the magnetic field was calculated based on the current intensity and the solenoid construction characteristics.

The following monovalent electrolytes were selected: lithium chloride, sodium chloride, and potassium chloride. Also, the divalent solutes of magnesium and calcium in the form of chlorides and acetates were used. The salts were ACS regent grade crystals. An analytic balance and DI water were prepared at 0.2 M, 0.05 M, and 0.1 M feed solutions. The concentration of each of the feed water solutions was calculated based on the measured conductivity.

Since the water permeability coefficient A and water diffusivity D_{WM} differs only by the constant $C_W V_W / RT\delta$ (assuming constant temperature), for practical purposes only A was calculated, based on experimental measurements. This parameter was used to evaluate the pure water diffusion coefficient within the membrane. The pure water permeability A was calculated using equation 1:

$$A = J_{PW} / P_1 = PWP / (S \cdot P_1) \qquad (1)$$

where J_{PW} was the pure water flux through the membrane ($mL \cdot min^{-1} \cdot cm^{-2}$), and it was calculated by dividing the measured pure water flow rate PWP milliliters per minute (mL/min) through the membrane by the total membrane surface area S square centimeters (cm^2), and P_1 was the operating pressure. The units for the pure water permeability coefficient, A, were ($mL \cdot min^{-1} \cdot cm^{-2} \cdot kPa^{-1}$).

The set of primary RO data included two measurable parameters (PWP and PR) and another one readily calculable based on experimental measurements (R). The measurable parameters were pure water permeation rate PWP (mL/min) through given area of membrane surface and product rate PR (mL/min) through given area of membrane surface. Based on the measured concentrations of salt in feedwater solution and in the product, rejection coefficient R was calculated using equation 2:

$$R = (C_{feed} - C_{product}) / C_{feed} \qquad (2)$$

Once the set of primary RO data was determined under the specified operating conditions of temperature, pressure, solute concentration in the feed solution, and feed flow rate, the salt permeation coefficient DK/δ was calculated using equations 3 to 5 derived from the preferential sorption-capillary flow model (known as Sourirjan's model). It should be emphasized that this model is largely used in the RO water treatment application, including seawater and brackish water desalination.

$$J_w = \frac{PR}{S \cdot \left(1 + \frac{m_{feed}(1 - R)M_S}{1000}\right)} \quad (3)$$

$$\Pi_{mem} = P_1 + \Pi_{prod} - \frac{J_W}{A} = nRTC_{mem} \quad (4)$$

$$\frac{D \cdot K}{\delta} = \frac{J_W}{\left(\frac{1 - X_{prod}}{X_{prod}}\right) \cdot \left(C_{mem} \cdot X_{mem} - C_{prod} \cdot X_{prod}\right)} \quad (5)$$

J_w is the water flux ($mL \cdot min^{-1} \cdot cm^{-2}$) which cannot be measured when the feed is a salt solution; M_S was the molecular weight of salt (g/mol); A is pure water permeability evaluated previously; and X_{mem} and X_{prod} were the salt mole fraction given by $X_i = C_i / (C_i + 55.5)$. The salt concentration at the membrane wall C_{mem} as well as the mole fraction X_{mem} in equation 5 were obtained from equation 4.

4. Results and Discussion

4.1 Acquisition of the Power Source

Difficulties were met in getting the appropriate power source that generates the magnetic field in the solenoid. In a first stage, a DC power source that provides currents up to 400 amperes (A) was made available by the USF Department of Electrical Engineering. However, the unit could not be used due to failure to accommodate the required input voltage (3 phase of 480 volts [V]) in the building where the experiments were set up. In a second stage (November 2001), an AC power supply was purchased from Behlman (model P1351). The source was found inadequate to generate the desired magnetic field. In the third stage, a power source was purchased in March 2002 from Georator Corporation. The Georator power source required a dedicated voltage line that was not available in the lab where the research was conducted. The dedicated line had to be installed.

The power source can generate a current up to 47 A at a frequency of 50 Hz and allows the possibility to vary not only the intensity of the magnetic field but also its frequency. The reasons of selecting this power source were as follows:

a) The AC source generates an electromagnetic field whereas a DC source can only provide a magnetic field with a constant magnitude for a given current. The electromagnetic field leaves the possibilities for further explorations of the effects on the salt transportation, as the electric component of the field may also play a role in the separation of the electrolytes.

b) The AC source with a large range for current variation was necessary to see how the reverse osmosis process reacts to different intensities of the electromagnetic field. This leaves the possibilities to observe if there is any threshold values of the electromagnetic field when certain effects occur.

c) The frequency of the electromagnetic field was another variable which can affect the transport of both water and salt across the RO membrane. The possibility of exploring the effects of a field at a set intensity but different frequency range must remain open.

The power supply for the electromagnetic field failed to function after the first 5 minutes of working due to unknown reasons. After several attempts to replace the fuses according to the manufacturer's instructions, it had to be sent back for repairs. This delayed the beginning of the tests with the magnetic field for another 4 weeks.

4.2 Results With the Survivor Unit

4.2.1 Pure Water Permeability in the Absence of ELMG Field

The Survivor unit was tested for a total of 42 hours divided in 9 tests. The pure water used as feed in this stage was made using a RO system with a capacity of 100 gallons per day (gal/day). Because the total membrane surface area, S, was not known from the manufacturer, the parameter $A \cdot S$ has been evaluated instead of A. This did not have any further implications for any stage of this project because first, S was constant, and second, to determine the concentration polarization and the solute permeability, $A \cdot S$ was needed. The overall pure water permeability, $A \cdot S$, has been calculated using equation 6 in order to evaluate the time τ necessary for the membrane to achieve a constant value of the pure water permeability.

$$A \cdot S = J_{pure\ water} / \Delta P \qquad (6)$$

For each test, $A \cdot S$ has been averaged for a period of 60 to 120 minutes after the system reached an equilibrium. Figures 1 and 2 represent the variation of the pressure and of the product flow for test 8. It should be noted that both the operating pressure and the product flow had sinusoidal variations that followed the strikes of the pump piston. Those variations do not represent errors in the instrumental readings. The pressure transmitter as well as the digital flowmeter for the permeate allowed the reading and recording of the data on a preset schedule, in this case of five samples per minute. For test 8, the overall pure water permeability $A \cdot S$ was obtained by applying equation 6 to all points for each $t > 200$ minutes, and then an average has been calculated.

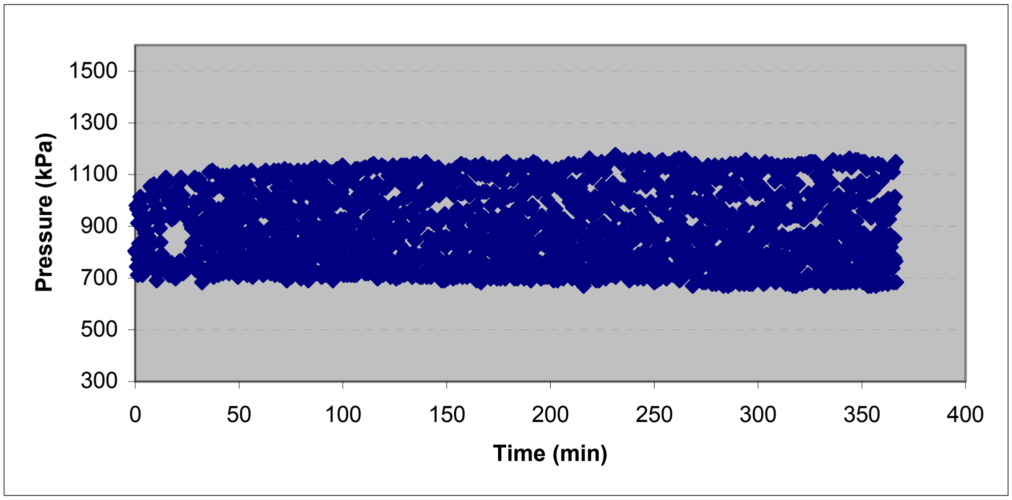

Figure 1. Variation of the operating pressure with time during test 8.

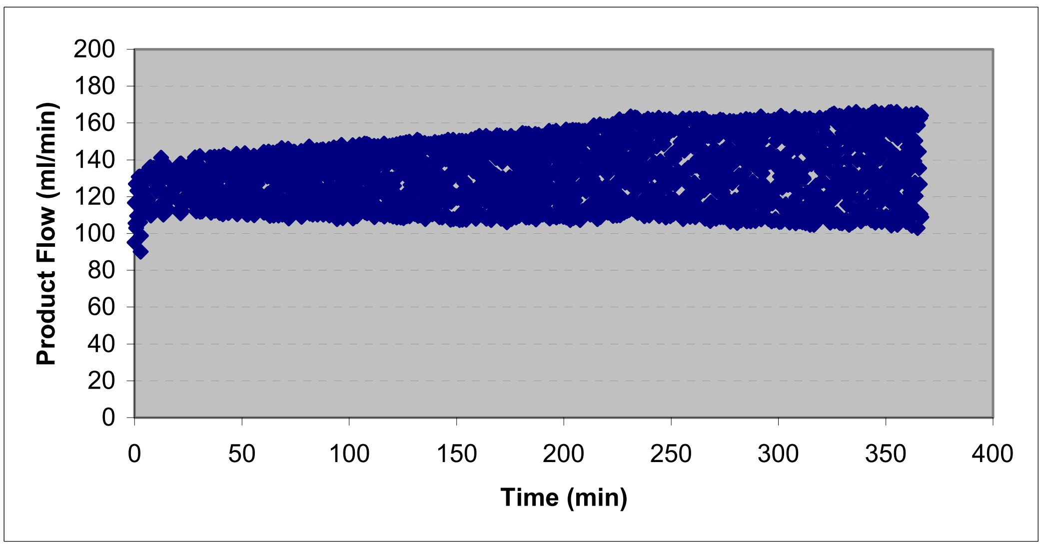

Figure 2. Variation of the product flow with time during test 8.

Figure 3 illustrates the dependence of the overall permeability A·S on feed temperature. The membrane seemed to reach a constant A·S after few hours of operation, however A·S was directly dependent on the temperature of the feed solution. Thus, a variation of 10.7% in the feed temperature for test 3 and test 9 corresponded to a variation of 9.1% in the pure water permeability. Moreover, figure 4 shows that A·S decreased with the increase in the operating pressure, probably due to the membrane compaction.

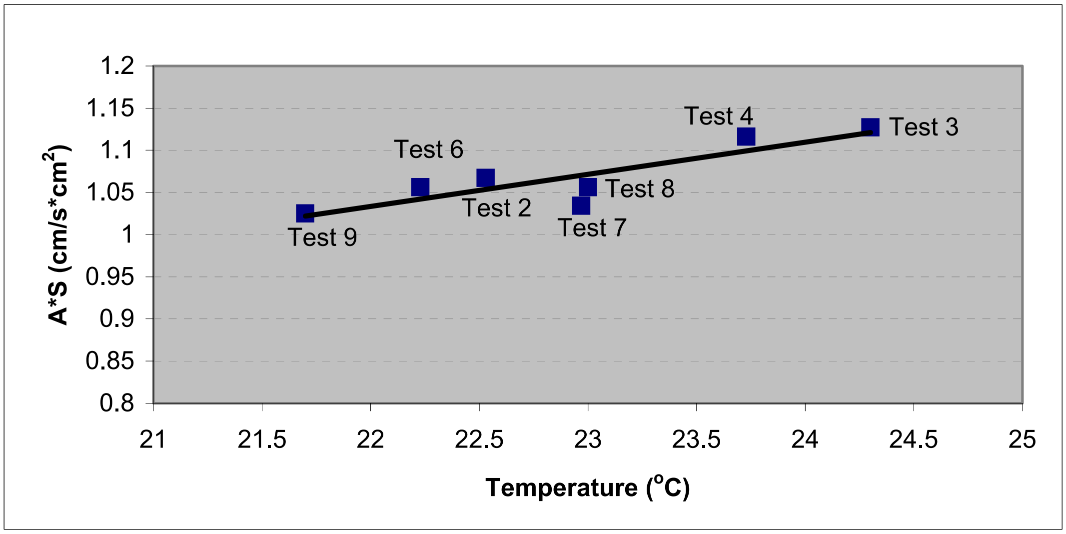

Figure 3. Dependence of the overall pure water permeability on temperature.

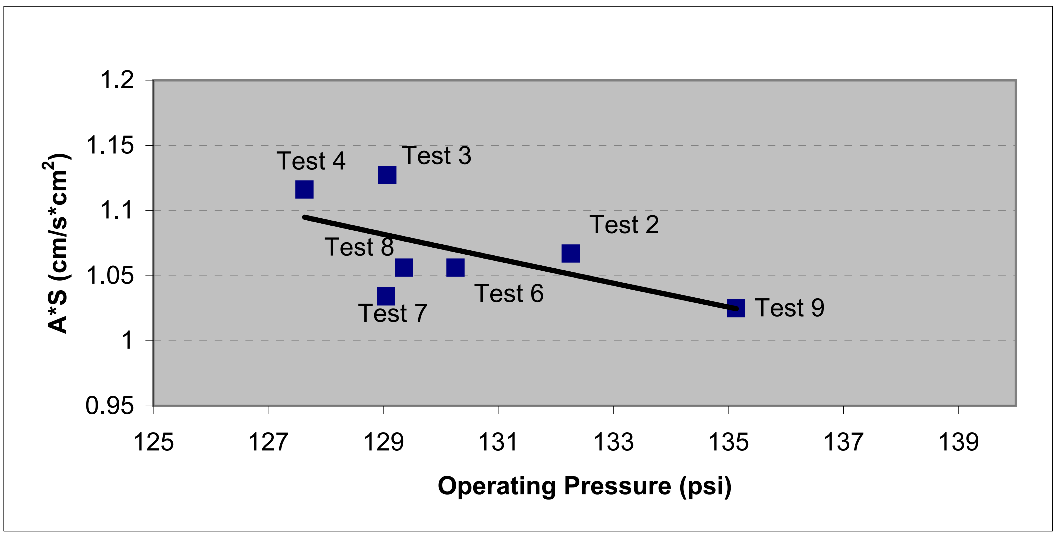

Figure 4. Dependence of the overall pure water permeability on the operating pressure.

The dependence of A·S on temperature and operating pressure was in agreement with the results reported in literature. Figures 3 and 4 show that both the feed temperature and the operating pressure had to be controlled in order to accurately evaluate the effects of magnetic fields on the salt transport.

4.2.2 Tests With NaCl and KCl at 0.02 M in the Absence of the ELMG Field

Although the conductivity sensors were new and according to the manufacturer, they did not require calibration, large errors have been encountered especially for readings of lower concentrations, such as the concentration of the product. A set of conductivity standards was purchased, and the errors were significantly reduced when the probes were calibrated for a range closer to the measured values.

Another problem came out when the mixer rod was introduced in the feed solution. The readings of the conductivity probe dropped by as much as 25% due to interference metallic rod – water – metallic plates of the probes. An attempt to solve the problem was by inserting the conductivity probe in the feed line. However, this caused a malfunction of the unit, which could not reach the pressure to produce the designed product flowrate. Since the system runs in a closed loop and the mixer assured a good homogeneity of the feed, an additional conductivity meter was used occasionally to check the feed concentration.

The pH probe that was inserted in the product-collecting bottle failed several times after few hours of operation. This was due to the low ions content of the product which determined a depletion in the ion content of the filling solution of the probe. The sensor was rehabilitated using the procedure described by the manufacture. However, as the pH of the product remains constant throughout a test, a hand-held pH meter was used for occasional measurements.

Preliminary tests were conducted for NaCl and KCl at two different feed concentrations, first at 0.02 M and second at 0.05 M. The objectives were the following:

a) Evaluate the dynamics of the system throughout a test, including variations in the feed temperature, operating pressure and product flow;

b) Calculate the differences in the salt permeability coefficient, DK/δ, and the mass transport coefficient, k, for NaCl and KCl for a constant feed concentration;

c) Evaluate the effects of the feed concentration on DK/δ and k for a certain salt;

d) Examine the differences in other parameters of interest (such as concentration polarization and rejection coefficient) for NaCl and KCl at constant feed concentration;

e) Evaluate the changes in the pure water permeability, A, due to long-term pressurization of the membrane.

The results are presented in table 1. The following observations were based on analysis of the data:

A. Dynamisc of the system

- As described in the operating manual, the RO unit "Survivor 35" operates by automatically increasing the pressure so that a constant product flow is delivered (constant recovery rate), regardless of the feed concentration and the salt; however, the product flowrate measured in all tests was about 20% less than what the manufacturer described: 68-69 mL/min versus 83 mL/min.

- An initial conditioning of the membrane occurred for the tests 1, 6, and 7 (which were completed in this order). In the conditioning stage, the operating pressure did not reach the optimal value, and the concentration at the membrane (concentration polarization) was continually increasing.

- For a certain salt and certain feed concentration, the variations in the feed temperature and, thus, the variations in the feed viscosity, were compensated by the variations in the operating pressure which adjusts so that a constant product flowrate was obtained. An illustration of this is presented in figures 5 and 6, where the values of the pressure and temperature represent averages over 15-minute intervals.

- During the longest tests (12 hours), the feed temperature has varied by less than 10%.

- For a feed concentration of 0.05 M, the operating pressure was higher for NaCl than for KCl. This can be explained by the development of a higher concentration polarization for NaCl than for KCl, and therefore a higher pressure was necessary to produce the same product rate.

Table 1. Results of the preliminary tests performed without the magnetic field

Test	Salt	Replicate #	Time hours	C feed mol/L	T feed °C	Pressure kPa	Flow P mL/min	C Product mol/L	R	C mem mol/L	$DK/\delta \times 10^7$ cm/s	$k \times 10^2$ cm/s
1	NaCl	1	4.2	0.02	20.1	1310	60.9	1.60E-04	99.2	0.044	14.8	3.33
2		2	10	0.02	21.9	1730	69.9	2.10E-04	98.9	0.104	7.64	1.48
3		3	4.2	0.02	21.3	1799	69.6	1.84E-04	99.0	0.116	7.73	1.55
4	KCl	1	10.9	0.02	22.3	1751	68.9	1.93E-04	99.0	0.103	8.39	1.59
5		2	2.9	0.02	21.5	1737	68	1.79E-04	99.1	0.110	7.66	1.57
6	NaCl	1	6.4	0.05	20.8	1717	70.4	4.71E-04	99.1	0.095	23.6	4.55
7		2	3.6	0.05	21.5	1730	70.1	5.10E-04	99.0	0.100	24.6	4.27
8		3	12	0.05	19.8	2206	68.4	6.23E-04	98.8	0.192	14.5	2.18
9		4	12	0.05	19.7	2123	68.9	6.22E-04	98.8	0.166	16.2	2.17
10		5	2.3	0.05	19.74	2110	68.7	5.50E-04	98.9	0.172	14.6	1.99
11	KCl	1	8.1	0.05	21.1	1992	68.2	5.78E-04	98.8	0.150	17.5	2.31
12		2	4	0.05	20.4	1992	68	5.61E-04	98.8	0.148	17.1	2.35
13		3	12	0.05	20.1	2068	69.4	4.90E-04	99.0	0.159	14.2	2.26

B. Salt permeability coefficient DK/δ:

- For both NaCl and KCl, the salt permeability depended on the feed concentration being higher for high feed concentrations.

- During a test, DK/δ varied inversely proportional with the operating pressure (figure 7).

- DK/δ was higher for KCl than for NaCl at both feed concentrations considered. However, the differences were small (less than 5% for 0.02 mole

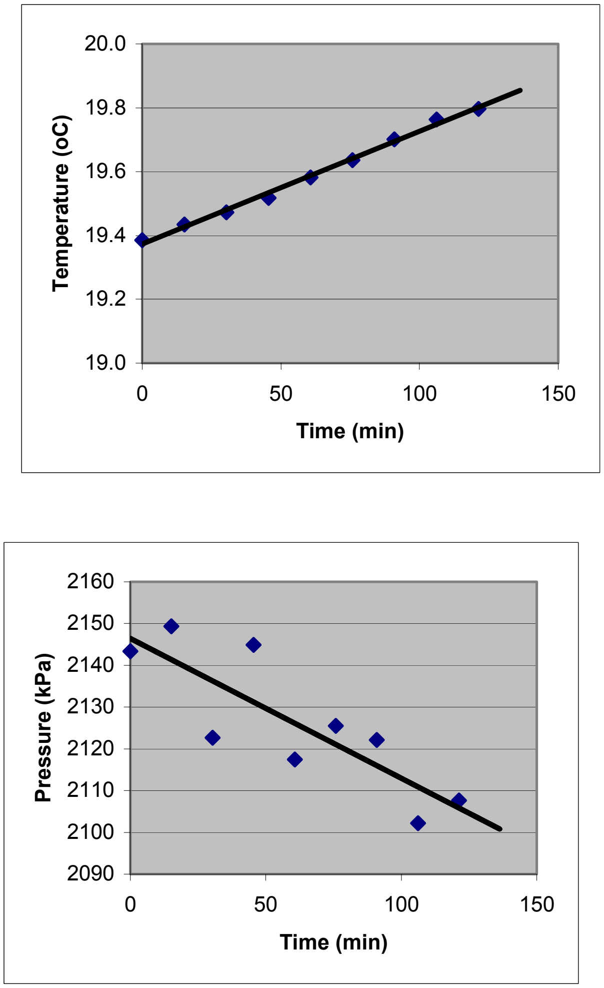

Figure 5. Pressure decreases with the increase in feed temperature in test 10.

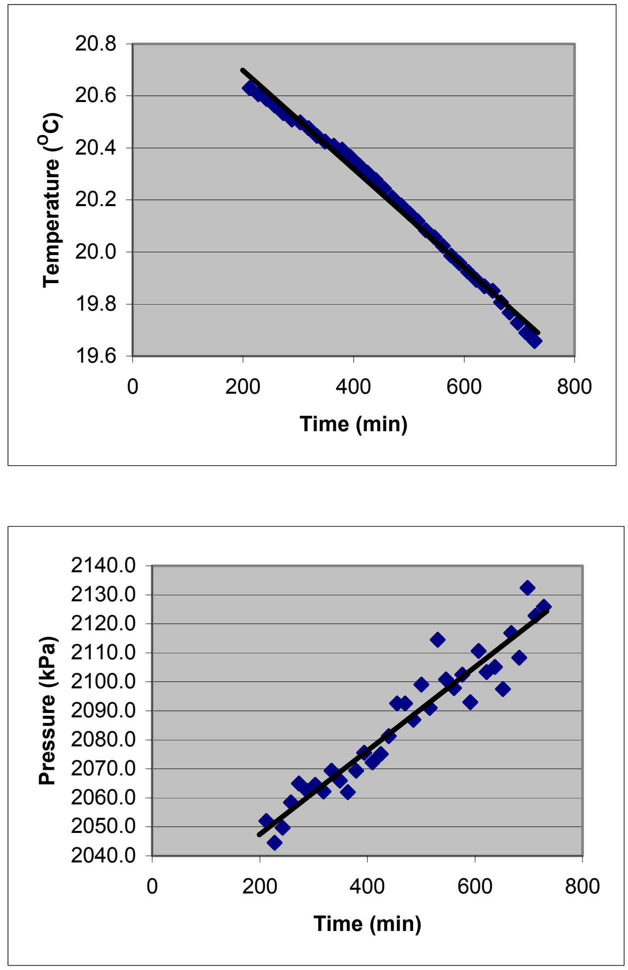

Figure 6. Pressure increases with the decrease in the feed temperature in test 9.

per liter (mol/L) and less than 8% for 0.05 mol/L) and were within the experimental error. It was believed that due to the very high membrane rejection (more than 98.8%), there was a small difference in the permeability of NaCl and KCl. Therefore, an increase in the feed concentration was necessary for the following tests.

C. Pure water permeability A

- The pure water permeability A declined in time (table 2), probably due to the membrane compaction under the prolonged exposure to pressure. The value of A had to be checked periodically to ensure that equilibrium has been reached.

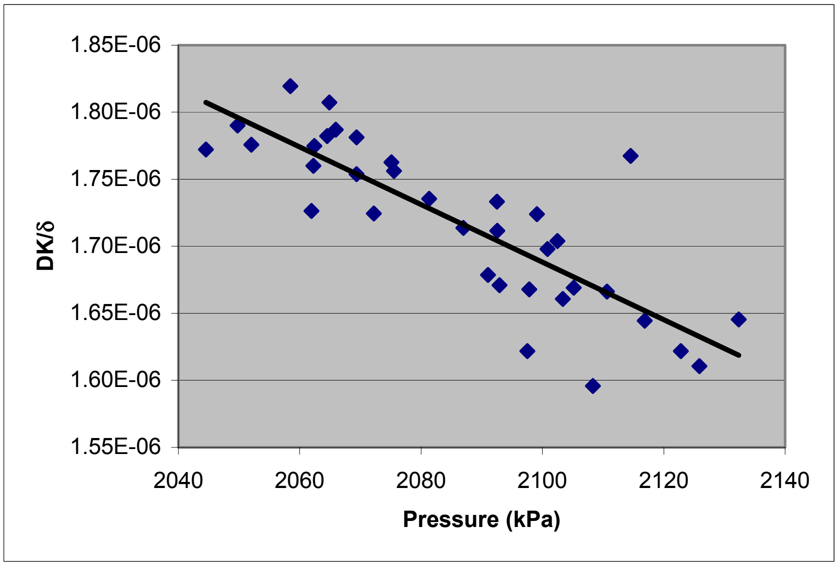

Figure 7. Dependence of salt permeability on the operating pressure in test 9.

Table 2. Pure water permeability after different tests

	T feed (°C)	**A x 10^4** ($ml{\cdot}min^{-1}{\cdot}kPa{\cdot}cm^{-2}$)
Before the salts	22.40	0.29
After test nr.10	22.45	0.21
After test nr. 13	20.60	0.20

D. Other parameters

- The rejection R remained close to 1 even for higher feed concentrations, and this explains why there was no difference in the rejection of NaCl and KCl.

- For a feed concentration of 0.05 mol/L, the concentration at the membrane was higher by about 16% for NaCl than for KCl. This result was explained by the higher hydration of Na^+ than of K^+, which determine an effective ionic radii greater for Na^+ than for K^+. Consequently, the accumulation of NaCl at the membrane wall was in larger quantities. This result was important for the potential of scale formation at the membrane surface.

- After the conditioning stage (tests 1, 6, and 7), the repeatability of the results was within 90%. Table 3 summarizes the average values of salt permeability and mass transport coefficient for tests after conditioning.

- The mass transport, k, in the feed side (characterizes the rate of salt transport from the membrane wall back to the feed solution) depends both on the feed concentration and the concentration at the membrane. Its reproducibility throughout the tests was more than 95% (table 3).

Table 3. The average values for the salt permeability and mass transport coefficient in the feed side

Salt	Conc Feed	DK/δ avg	k avg
NaCl	0.02	7.7±0 .8%	1.5±3.3%
KCl	0.02	8±6.4%	1.6±0.9%
NaCl	0.05	14.4±10.4%	2±5.5%
KCl	0.05	15.7±9%	2.2±0.8%

The following were concluded for this stage of the project:

1. Although the rejection of salt R was constant for both NaCl and KCl, the differences in salt permeability were reflected in the operating pressure and the concentration polarization, with KCl going faster through the membrane. It was believed that by increasing the feed concentration, a better differentiation between the transport parameters for NaCl and KCl can be observed.
2. The pure water permeability A has to be determined periodically, a convenient time for checking being whenever the cleaning between different salts was performed.
3. The RO system reaches stability within 1 hour from the beginning of a test; however, the feed temperature was an important factor in determining the operating pressure and, further, the entire dynamic of the system. Thus, a very good monitoring and control of the temperature of the feed and product was necessary to evaluate the effects of the electromagnetic field and to ensure that those effects were not hidden by the temperature effects.
4. To remedy the low product flow obtained for all tests, a complete set of o-rings and check valves were purchased and replaced before the next stage of the project was begun.

4.2.3 Tests With All Salts at 0.1 M With/Without ELMG Field

Consequently to the replacement of the o-rings and the check valves with the available Repair Seal Kit, the product flowrate increased to 98% of the designed value (from 83% previously reported). Table 4 presents the values of the product flowrate for all the studied salts in the absence of the magnetic field.

The increase of the feed concentration from 0.05 M to 0.1 M emphasized, to a larger extent, the differences in the salt permeability coefficient DK/δ for the analyzed salts, as shown in table 4. The rejection coefficient R remained almost the same for all salts; and, therefore, it cannot be used in the investigation of salt transport.

Table 4. System parameters and salt transport parameters at 0.1 M in the absence of the field

Test #	Test Replicate	Salt	T Feed °C	Conc. Feed mol/L	Conc. Product mol/Lx10^{-3}	Flow Prod ml/min	P kPa	R %	C_{mem} mol/l	DK/δ cm/sx10^{-6}
7	1	LiCl	19.8	0.1	1.00	80.9	2461	98.9	0.170	3.1
8	2	LiCl	20.1	0.1	1.00	79.8	2361	98.9	0.154	3.62
17	3	LiCl	20.2	0.1	1.06	82.9	1896	98.8	0.05	12.3
1	1	NaCl	20.6	0.1	1.02	80.1	2292	99.0	0.138	3.9
5	2	NaCl	20.2	0.1	0.96	80.9	2203	98.9	0.117	4.34
6	3	NaCl	20.1	0.1	1.03	80.8	2192	98.8	0.115	4.78
15	4	NaCl	20.1	0.1	1.16	81.9	1875	98.8	0.05	14.2
2	1	KCl	20.4	0.1	1.05	80.8	2137	98.9	0.104	5.4
3	2	KCl	20.2	0.1	1.06	81	2103	98.9	0.096	5.92
4	3	KCl	20.2	0.1	1.11	81.2	2089	98.7	0.092	6.49
14	4	KCl	20.2	0.1	1.13	82	1792	98.8	0.03	22.7
9	1	$MgCl_2$	19.8	0.1	0.96	79.1	2833	99.0	0.250	1.97
10	1	$CaCl_2$	20.0	0.1	0.90	80	2440	99.0	0.17	2.76
16	1	LiAc	20.1	0.1	0.81	81.9	1939	99.2	0.06	7.8
11	1	NaAc	20	0.1	0.78	81.6	1994	99.2	0.072	5.8
18	2	NaAc	20.1	0.1	0.75	81.9	1732	99.2	0.03	11.1
12	1	KAc	20.2	0.1	0.83	81.3	1933	99.1	0.06	7.5
13	2	KAc	20.1	0.1	0.81	81.5	1889	99.2	0.05	8.81

Notes: (1) The first column of represents the chronological order of the tests.
(2) The shaded rows represent tests with unexpected low operating pressure, which resulted in errors such as smaller concentration at the membrane wall than the concentration in the feed. Those tests were not considered for discussion in this paragraph; however, the issue was addressed under the paragraph "B. Reproducibility of the tests."

4.2.3.1 Tests Without the Magnetic Field

A. Importance of ionic radii, hydrated radii, and ionic charge

As described previously, the RO unit Survivor 35 operates by automatically increasing the pressure until a constant product flowrate is obtained. Thus, the greater a salt was rejected, the higher was the concentration at the membrane wall and the higher was the operating pressure. The salt permeability DK/δ indicates the following order of transport for the chloride salts (tests 1 through 5, table 4):

$$MgCl_2 < CaCl_2 < Li\,Cl < NaCl < KCl$$

For cations with the same ionic charge, one should note that larger ions (such as K) permeated faster through the membrane than smaller ions (such as Li). This contradiction can be explained if one considers the hydrated radii of the ions rather than the crystallographic one. Due to the dipolar nature of the water molecules, the dissociated cations form new aggregates consisting of a shell of

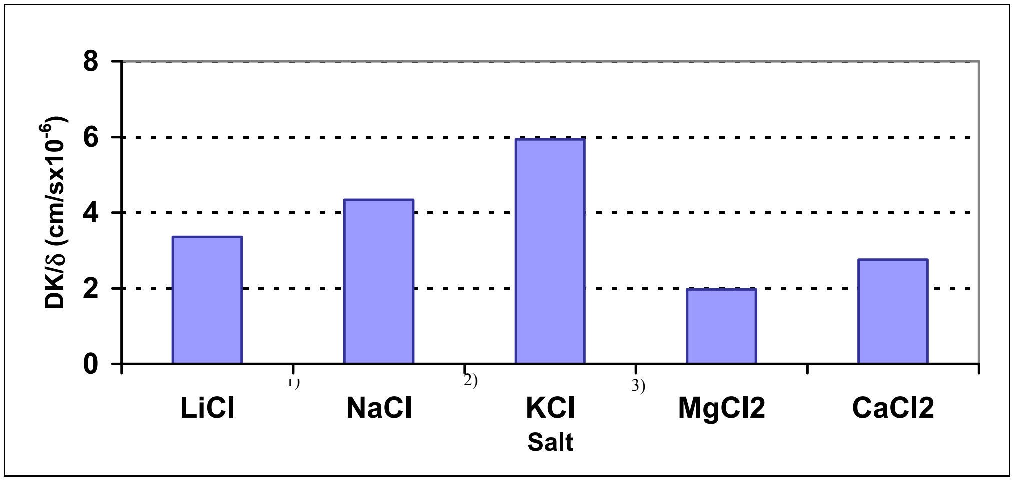

Figure 8. Salt permeability for chlorides of monovalent and divalent ions.

Notes: [1] Averages of replicates 1 and 2.
[2] Averages of replicates 1 to 3.
[3] Averages of replicates 1 to 3.

water molecules known as water of hydration surrounding the ion. The smaller the ionic radii of ions and the bigger the electric charge, the stronger the interaction with the water molecules and Acronym defined, consequently, the larger the hydrated radii. Figure 9 shows good correlation of DK/δ with the hydrated radii. This indicates that the ions maintain their hydration to a certain extent while crossing the membrane.

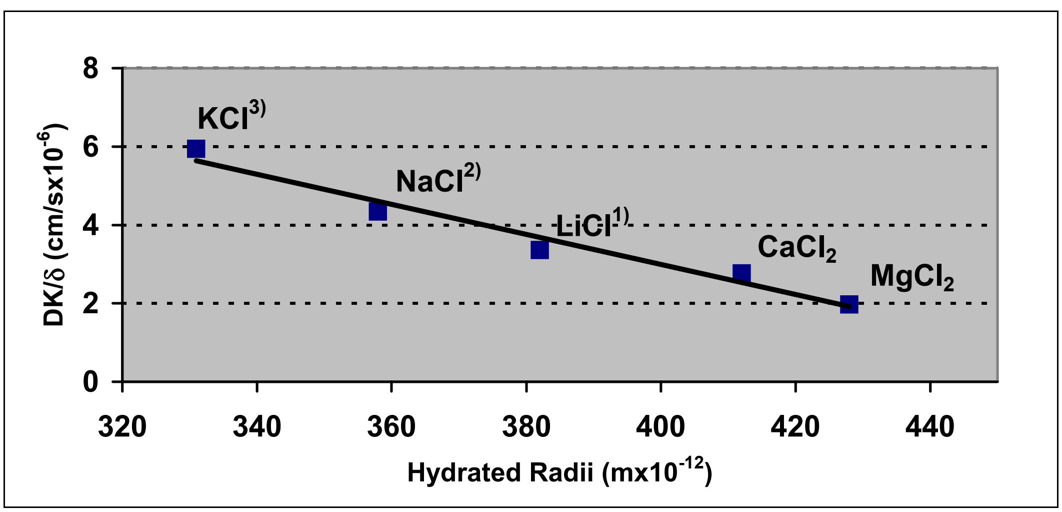

Figure 9. Dependence on salt permeability on the hydrated radii.

The effect of the ionic charge on the salt permeability was presented in figure 10 by comparing two pairs of cations with very close radii but different charge (Li

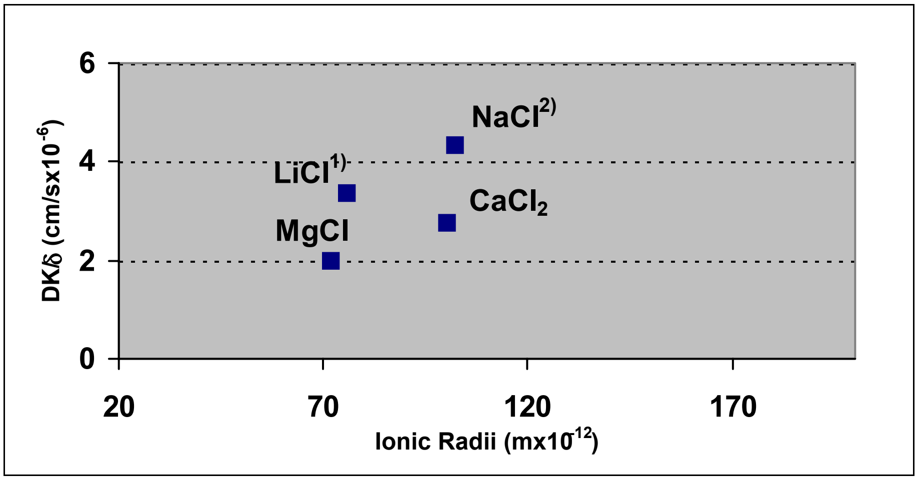

Figure 10. Dependence on salt permeability on the ionic radii.

versus Mg and Na versus Ca). Thus, the divalent ions Ca^{2+} and Mg^{2+} were rejected in a larger extent than the monovalent ions Na^+ and Li^+.

B. Reproducibility of the tests

The operating pressure presented unexpected variation even for replicates test one after another (for example, NaCl #5 and 6 or KCl #2 to 4). The pressure dropped for each replicate of the five studied salts. The further in time a replicate test was performed from the original test, the greater the variation in operating pressure (e.g., LiCl #17, NaCl #15, or KCl #14 which were all test after the acetates salts).

The drop in the pressure could have been determined by two sources: (1) there was a real pressure drop along the pressure vessel and the differential pressure increases as the salt was accumulated continuously at the membrane wall (concentration polarization) (2) the pressure measured was not the true operating pressure. Since the initial design of the RO-Survivor 35 did not include any point of pressure measurement, a pressure gauge and a pressure transmitter were added at the concentrate side (figure 11). However, the RO-Survivor 35 was designed so that the concentrate was not released immediately at atmospheric pressure, but it was turned behind the pump piston, for energy saving purposes. Regardless the case of the pressure drop, there was no other available point where the pressure can be measured and/or controlled.

Consequent to the variation in the operating presure, the calculated salt permeability coefficient DK/δ increases to a large extent. For example, in the case of KCl, a variation of pressure by 19.2% corresponds to a variation of DK/δ by 320%. It was believed that the large variations in the salt permeability were solely due to the errors in the pressure readings, and modifications of the RO system were required at this point. Other measured parameters, such as feed temperature, concentration of the product, and the flowrate of the product, were well reproducible.

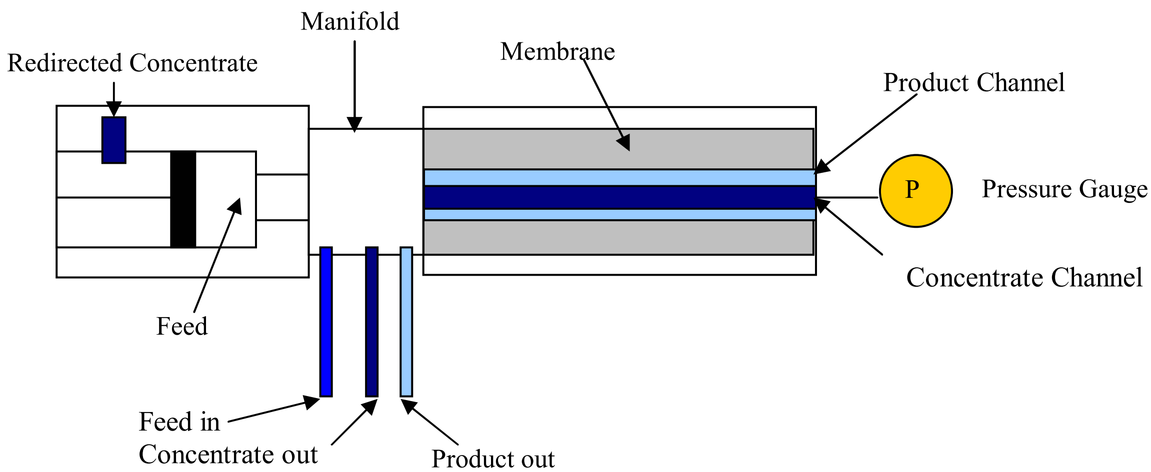

Figure 11. Schematic diagram of the RO-Survivor 35.

4.2.3.2 Tests With the Magnetic Field

After approximately 10 hours of tests with the applied electromagnetic field, cracks appeared in the pressure vessel due to the high temperatures developed inside the solenoid. The water leakages from the pressure vessel were small, from 1 to 10 grams of water for a test of 4-5 hours. Under these circumstances, seven alternative tests with/without magnetic field were performed for NaCl at a feed concentration of 0.1 M, and the results are presented in table 5.

Table 5. Tests with/without magnetic field for 0.1 M NaCl

Test #	**ELMG Field**	**T Feed** °C	**Concentration Product** mol/Lx10^{-3}	**Flow Product** mL/min	**T Product** °C	**P** kPa	**DK/δ** cm/sx10^{-6}
1	OFF	19.3	1.14	78.1	20.2	2111	5.37
2	ON	19.3	1.26	79.3	23.2	2025	7.60
3	OFF	22.6	1.24	74.9	23.2	2546	2.87
4	ON	19.6	1.18	75.2	23.2	2695	2.41
5	OFF	22.4	1.28	72.3	23.2	2505	2.83
6	ON	18.8	1.24	70.4	23.4	2658	2.26
7	ON	18.2	1.27	71.95	23.3	2738	2.27

When the magnetic field was applied (the current applied to the solenoid was 24A), the product temperature was about 3 °C more than the product temperature for the tests with no magnetic field (tests 1 and 2). Moreover, figures 12 and 13 present a strong correlation between the product conductivity and the product temperature (the conductivity sensors have automatic temperature compensation). For example, in figure 12, when the temperature drops to its lowest value of 21.6 °C, at 56 minutes, the conductivity is also at its lowest value of 150 µS/cm.

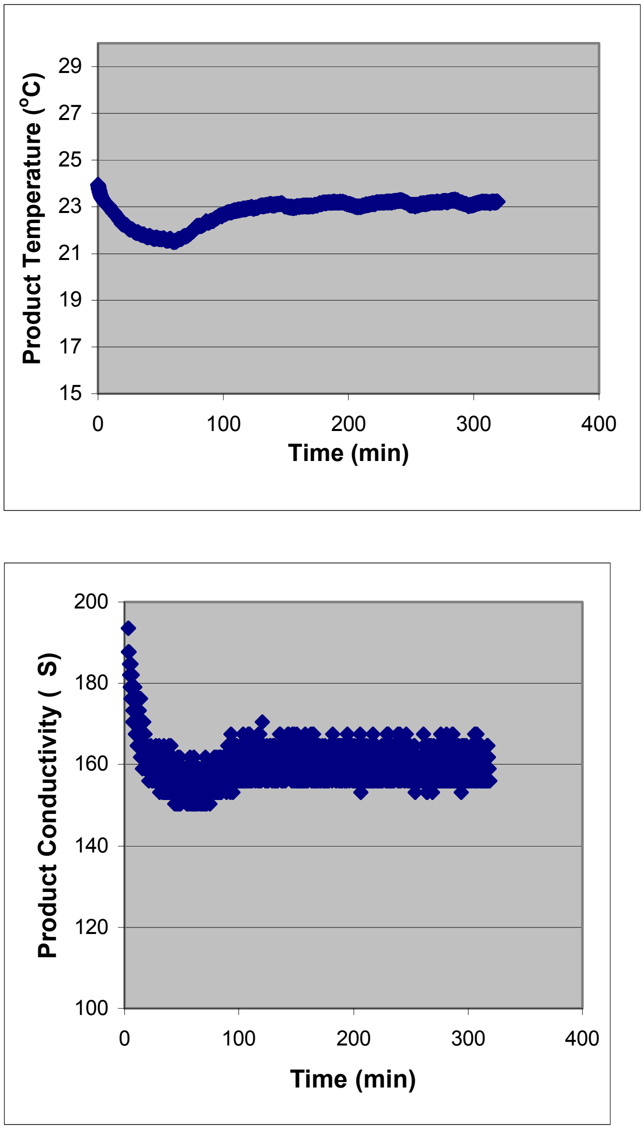

Figure 12. Dependence of product conductivity on the product temperature in test 2.

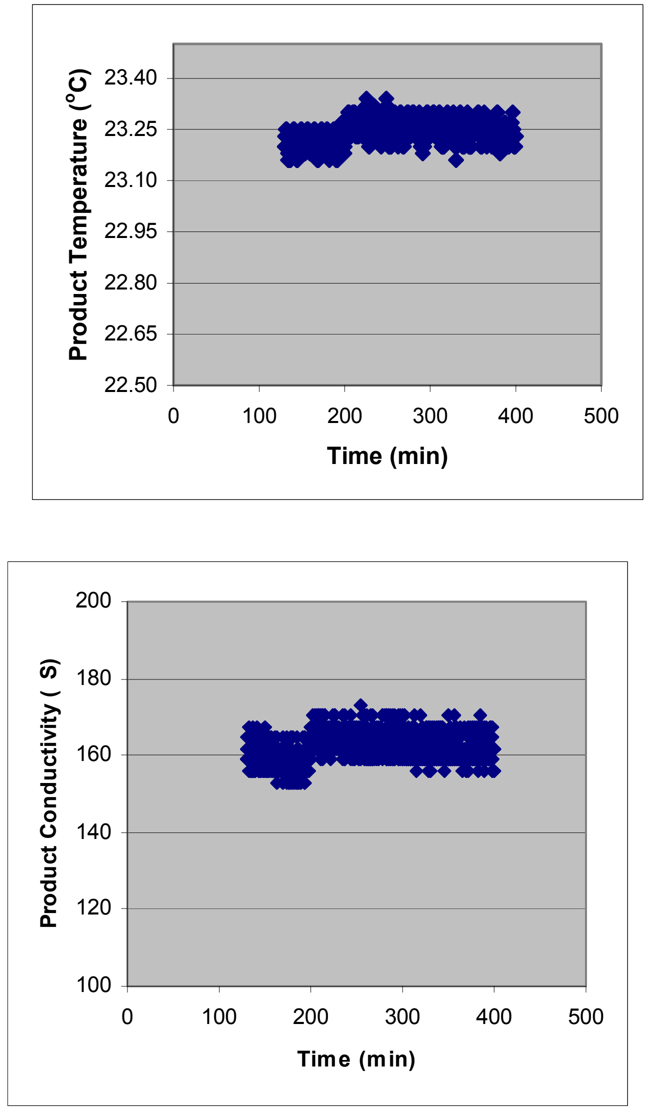

Figure 13. Dependence of product conductivity on the product temperature in test 5.

Since diffusion plays an important role in the mechanism of salt transport through the membrane, the variation of product conductivity with temperature can be explained by the dependence of diffusivity rate on temperature. One attempt to overcome the temperature differences in the product was performed by increasing the feed temperature for the tests with no field until the product reached the same temperature as for the tests with the field applied (i.e., increase the feed temperature from 19.3 °C to 22.6 °C).

Table 6 presents the average values of the parameters which characterize the salt transport of NaCl with/without the electromagnetic field, together with feed temperature and pressure. The salt permeability, DK/δ, decreased by 23% when the field was applied. However, since DK/δ was shown to depend on the pressure (figure 7), there were two reasons that make uncertain whether the decrease in

Table 6. Product concentration and salt permeability for tests with/without electromagnetic field

ELMG Field	T Feed (°C)	P (kPa)	Product Concentration (mol/L x 10^{-3})	DK/δ (cm/s x10^{-6})
OFF[1]	22.5	2525	1.26	2.85
ON[2]	18.9	2697	1.23	2.31

Notes: [1] Averages for tests 3 and 5.
[2] Averages for tests 4, 6, and 7.

DK/δ was an effect of the applied electromagnetic field: (1) as described earlier in this report, the measured pressure might not be the real operating pressure, and (2) there was a dependence of the pressure on the feed temperature—a decrease in feed temperature corresponds to an increase in the pressure, as shown in figures 4 and 5.

Since the operating pressure and the product temperature could not be controlled (the operating pressure due to auto-regulating pressure for the Survivor unit, and the product temperature due to the heat generated by the electromagnetic field), the current RO system was inadequate for examining any field effects. Moreover, the jump up of the pressure starting with test 3 together with the continuous drop of the product flowrate indicated that the cracks were enlarging and the need for a new RO/Electromagnetic field system was essential.

There were several critical points that a new experimental design has to meet: 1) capability of pressure control and certainty of measuring the real operating pressure; 2) capability of controlling the product temperature; and 3) prevent overheating of the solenoid, especially in the inner part where the pressure vessel was located. The excessive heat may not only produce cracks in the pressure vessel but also may affect the membrane properties.

Drawings of the proposed RO experimental apparatus are included in the Appendix, together with a list and a brief characterization of the system components. The operating pressure in the modified RO system was controlled by a needle valve placed on the concentrate side. A pressure gauge and a pressure transmitter were mounted on the reject line, before the needle valves. The control of the product temperature and the prevention of the solenoid overheat were managed by a cooling system. It consisted of a cupper tubing wound on the pressure vessel. Cold tap water was circulated through the cupper tubing. Air was blown by a fan through an air gap of ½ inch which spaced the tubing from the solenoid.

4.3 Results With the Modified RO System

The proposed new system has proved to be adequate for controlling and measuring the operating pressure. The system was very stable; and in less than 1 hour, the operating pressure and the product flow reached equilibrium. The increase of the product temperature due to magnetic field was small (within 1 °C) comparing with the previous system, for which the increase in the product temperature was up to 4 °C. The winding of the electromagnetic coil on a separate pipe than the pressure vessel assured a sufficient air gap to protect the pressure vessel from overheating. The cooling system mounted between the pressure vessel and the pipe supporting the coil provided additional temperature-rise protection for the pressure vessel.

4.3.1 Tests With All Salts at 0.05 M With/Without the ELMG Field

The membrane was initially conditioned for 10 hours using 0.05 M solution of NaCl. The tests with the salts were performed consecutively, i.e., starting with LiCl and ending with $CaCl_2$ as presented in table 7. After each test, the system was flushed with tap water for 1 hour. Each salt solution has a concentration of 0.05 M, and the operating pressure was 260 pounds per square inch (psi). The feed water was maintained at 23 °C. Each solution test for 3 hours without the field ("No Field" in table 7), then 90 minutes with a field of approximate 680 Gs at 40 Hz ("Field 1" in table 7), followed by 90 minutes with a field of approximate 680 Gs at 300 Hz ("Field 2" in table 7). The pure water permeability A was measured following the same schedule with/without the field as for the salt solutions. The tests for the pure water were carried out three times as follows: after the conditioning period, after all the salts were tested first, and after all the salts were tested for the second time. The results for A were presented in table 8 and figure 14.

As shown in table 7, there were no significant changes in the salt rejection, product flowrate normalized to pressure J_p and salt permeability DK/δ when the electromagnetic field was applied, either at 40 Hz or 300 Hz. There were no

Table 7. System parameters and salt permeability at 0.05 M with/without the ELMG field

Salt	Field	Test 1				Test 2			
		(°C)	R %	J_p (mL·min^{-1}·kPa^{-1})	DK/δ (cm·s^{-1})	T prod (°C)	R	J_p (mL·min^{-1}·kPa^{-1})	DK/δ (cm·s^{-1})
LiCl	No Field	23.2	99.38	1.49E-05	2.64E-06	23.2	99.45	1.57E-05	2.25E-06
	Field 1	23.6	99.35	1.48E-05	2.62E-06	23.6	99.44	1.57E-05	2.27E-06
	Field 2	23.9	99.34	1.48E-05	2.63E-06	23.9	99.43	1.57E-05	2.29E-06
NaCl	No Field	23.2	99.37	1.49E-05	2.65E-06	23.2	99.51	1.60E-05	2.10E-06
	Field 1	23.6	99.35	1.49E-05	2.65E-06	23.6	99.48	1.60E-05	2.20E-06
	Field 2	23.9	99.34	1.49E-05	2.65E-06	23.9	99.46	1.58E-05	2.19E-06
KCl	No Field	23.2	99.24	1.52E-05	3.52E-06	23.2	99.32	1.61E-05	2.99E-06
	Field 1	23.6	99.22	1.52E-05	3.52E-06	23.6	99.3	1.61E-05	3.08E-06
	Field 2	23.9	99.22	1.52E-05	3.56E-06	23.9	99.29	1.61E-05	3.17E-06
$MgCl_2$	No Field	23.2	99.48	1.41E-05	1.48E-06	23.2	99.52	1.47E-05	1.31E-06
	Field 1	23.6	99.42	1.40E-05	1.60E-06	23.6	99.49	1.47E-05	1.34E-06
	Field 2	23.9	99.42	1.39E-05	1.55E-06	23.9	99.49	1.47E-05	1.37E-06
$CaCl_2$	No Field	23.2	99.42	1.39E-05	1.62E-06	23.2	99.48	1.44E-05	1.35E-06
	Field 1	23.6	99.41	1.39E-05	1.65E-06	23.6	99.47	1.44E-05	1.39E-06
	Field 2	23.9	99.4	1.39E-05	1.69E-06	23.9	99.45	1.43E-05	1.40E-06

Table 8. Feed and product temperature and pure water permeability with/without the field

ELMG. Field	After Conditioning			After Test 1			After Test 2		
	T feed	T prod	A x 10-4	T feed	T prod	A x 10-4	T feed	T prod	A x 10-4
	(°C)	(°C)	(mL·min-1··kPa-1·cm-2)	(°C)	(°C)	(mL·min-1··kPa-1·cm-2)	(°C)	(°C)	(mL·min-1··kPa-1·cm-2)
No Field	23.0	23.2	0.18	23.0	23.2	0.19	23.0	23.2	0.19
Field 1	23.0	23.6	0.18	23.0	23.6	0.19	23.0	23.6	0.19
Field 2	23.0	23.9	0.18	23.0	23.9	0.19	23.0	23.9	0.19

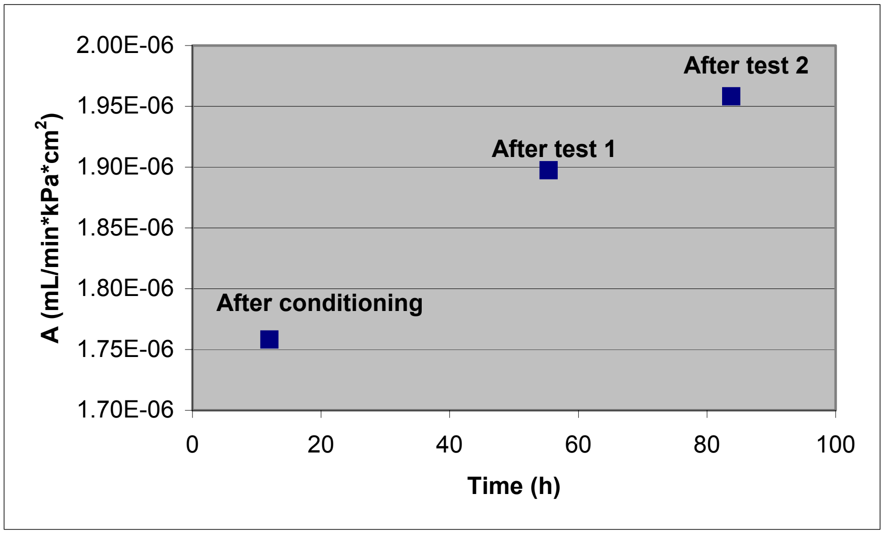

Figure 14. Variation of pure water permeability in time.

changes in the pure water permeability, A, when the field was applied (table 8). However, as shown in figure 14, the pure water permeability increased for the overall duration of 84 hours.

In order to identify whether the observed changes from test 1 to test 2 for the pure water permeability were due to electromagnetic field, a modification of the original schedule of the tests was presented in table 9. Since it was expected that the electromagnetic field affects the membrane potential for scaling/fouling, time and feed concentration were factors to be mainly considered. The new set of tests was performed with feed solution of $CaCl_2$, 0.1 M, and the total duration of the tests was approximately 408 hours. Tests 2, 4, and 6 were performed without the electromagnetic field, and tests 8, 10, and 12 were performed with the electromagnetic field. The electromagnetic field was 680 Gs at 40 Hz. Tests for the pure water permeability were performed in the absence of the field.

4.3.2 Tests With $CaCl_2$ at 0.1 M With/Without ELMG Field

The pure water permeability A from the new set of tests was presented in figure 15 together with A from the previous tests of the modified RO system

Table 9. Schedule of the last set of tests

Test #	Nr. of Hours	Feed	Electromagnetic Field
1	3	DI	off
2	68	$CaCl_2$, 0.1M	off
3	3	DI	off
4	68	$CaCl_2$, 0.1M	off
5	3	DI	off
6	68	$CaCl_2$, 0.1M	off
7	3	DI	off
8	68	$CaCl_2$, 0.1M	ON
9	3	DI	off
10	68	$CaCl_2$, 0.1M	ON
11	3	DI	off
12	68	$CaCl_2$, 0.1M	ON
13	3	DI	off

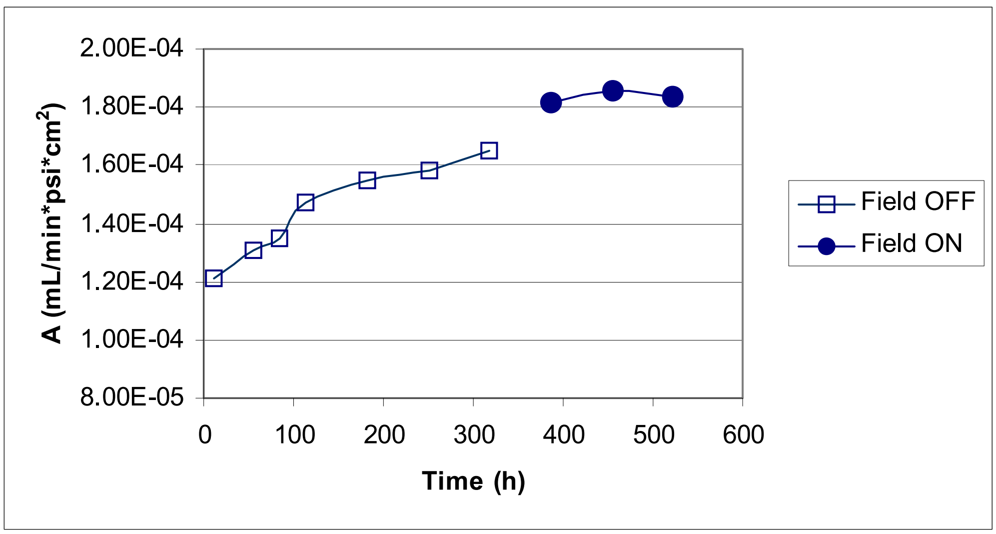

Figure 15. Variation of pure water permeability in time for the new system.

(figure 14). The continuous increase of A suggested that the membrane did not reach the equilibrium condition after more than 500 hours. The values of A following a salt test with a field (tests 9, 11, and 13) were higher than the values of A following a salt test with no field (3, 5, and 7). It is uncertain whether this difference is due to the electromagnetic field or due to the fact that the membrane did not reach an equilibrium.

The salt permeability DK/δ increased for the first three tests with the salt when no field was applied, and it decreased for the last three tests with the salt when the

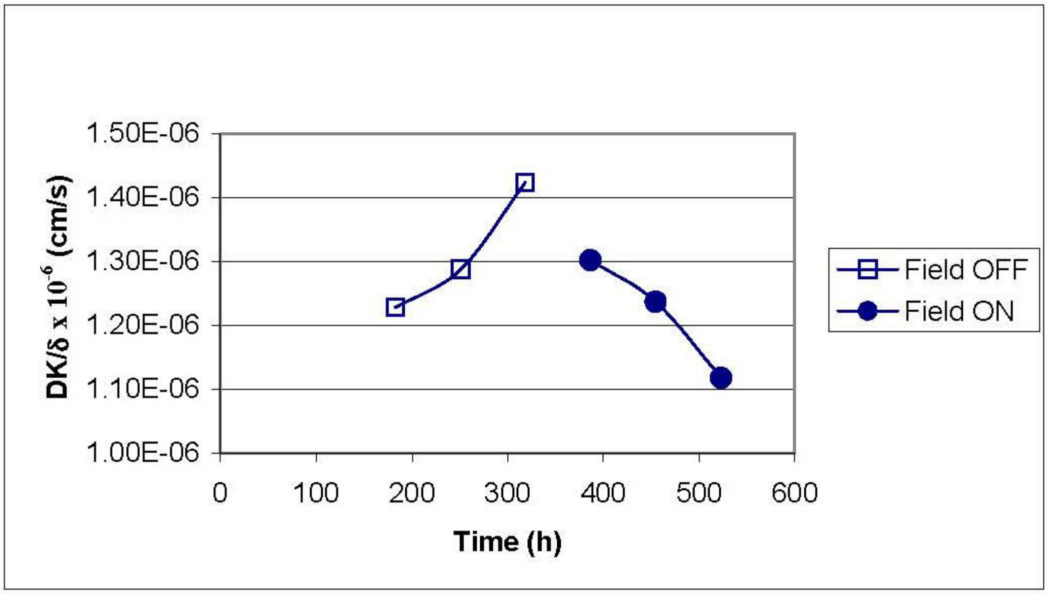

Figure 16. Variation of the salt permeability in time for the new system.

field was applied (figure 16). In average, DK/δ with the field on was 7% lower than DK/δ with no field. The difference is within the experimental error.

Figure 17 presents the variation of the product flow normalized to the operating pressure for the tests with salts from table 9. The increase in the normalized product flow followed by its decline suggested that the membrane has reached and passed the equilibrium stage and it started the regime of scaling formation corresponding to a continuous decline of the normalized product flow. Consequently, the increase in A and the decrease of DK/δ when the field was applied (figure 16) was believed to be an effect of the electromagnetic field.

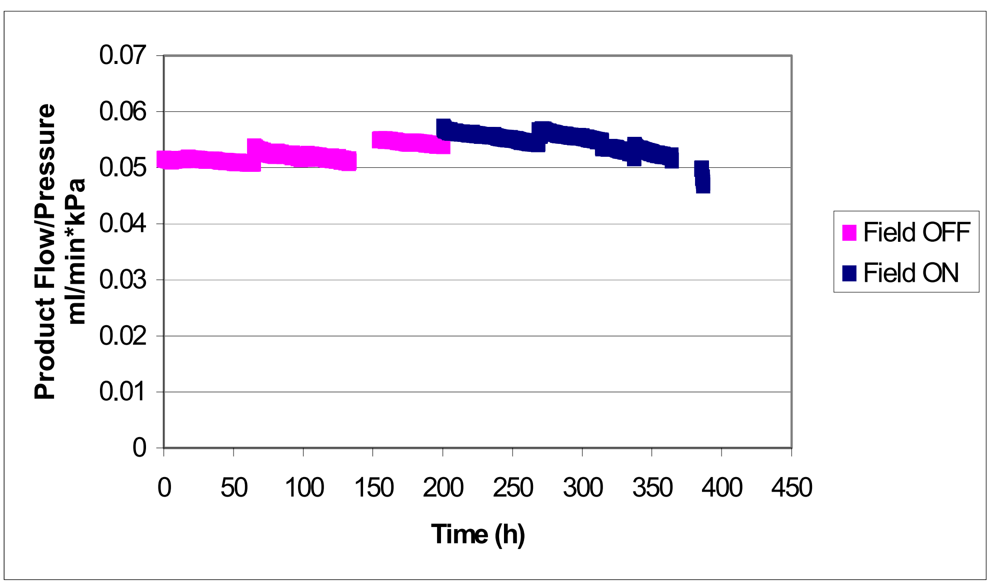

Figure 17. Variation of the product flow normalized to pressure in time for the last set of tests with the new system.

Figure 18 presents the variation of the product concentration in time. Similar to figure 17, the increase of the product concentration in time suggested that the membrane had passed the equilibrium stage and started the regime of scaling formation corresponding to the decrease in the membrane rejection.

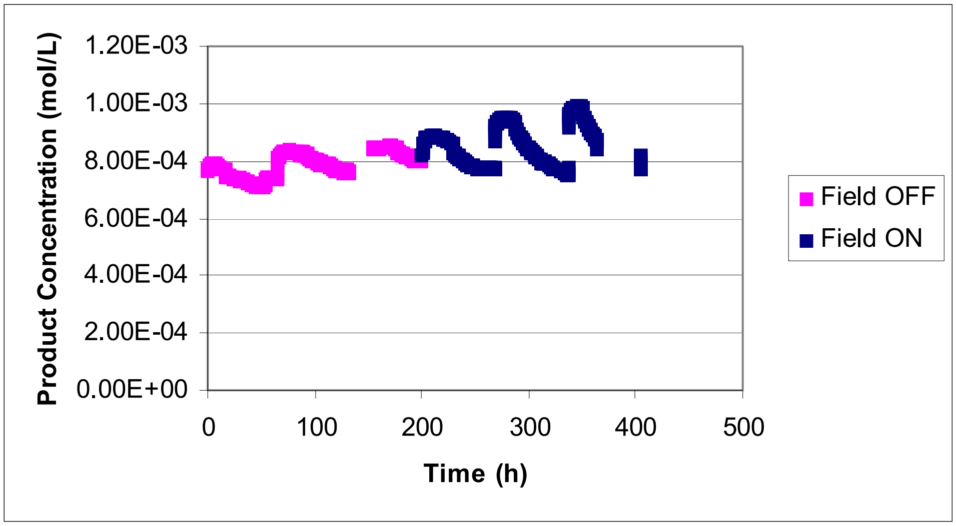

Figure 18. Variation of the product concentration in time for the last set of tests with the new system.

5. Summary and Conclusions

The effect of the electromagnetic field on the salt transport in RO membranes was studied using two experimental apparatus: the first one, referred to as Survivor unit, and the second one, referred to as the modified RO system. In both systems, the electromagnetic field was generated by a solenoid wrapped around the membrane pressure vessel. The Sourirajan's model was used to calculate the salt permeability DK/δ.

Several problems were encountered in the beginning of the project. The project was delayed initially by the difficulties in acquiring the appropriate current source for the solenoid because an AC current of at least 40 A was desired. Also, the current source had to be capable to allow the variation of both current intensity and current frequency. The power source failed after less than 5 minutes of testing, and it was sent back for repairs. Additional problems were encountered with the sensors for conductivity and pH. Errors in the conductivity sensor readings of the feed concentration were observed due to interferences with the metallic rod used for mixing. The pH sensor for the product failed repeatedly after few hours of taking measurements.

The initial pure water and salt solutions tests with the Survivor unit with no field revealed the importance of temperature and pressure control for the operating system. The tests with NaCl and KCl at 0.02 M and 0.05 M showed that a higher concentration in the feed solution was desired to better reflect the differences in the salt transport of the two salts. At this phase of the project, the o-rings and the check valves had to be replaced for the Survivor because the unit did not function at the designed parameters (it provided a lower recovery rate).

The tests with LiCl, NaCl, KCl, $MgCl_2$, and $CaCl_2$ at 0.1 M with no field showed that a certain order of the salt permeability was established among the five salts. The permeation rate increased in the order $MgCl_2$ < $CaCl_2$ < Li Cl < NaCl < KCl which can be explained by the degree of hydration for the cations. The replicates of the above salt solutions presented unexpected large variations for the operating pressure. These variations suggested that the readings of the operating pressure were improper, because of the locations of the pressure gauge and the pressure transmitter.

When an electromagnetic field was applied to the Survivor unit, the temperature of the product increased by about 3 °C. The increased in the product temperature when the field was applied made difficult the comparison of DK/δ with and without the field, because the effects of the field could not be separated from the effects of the temperature. Moreover, after about 10 hours with the electromagnetic field, cracks appeared in the pressure vessel due to high temperature developing inside the solenoid. All these led to the decision to change the experimental apparatus.

The modified RO system had the capability to control the operating pressure; and since a cooling system was placed between the solenoid and the pressure vessel, the temperature of the product varied by less than 1 °C when the field was applied. Chloride solutions of Li, Na, K, Mg, and Ca at 0.05 M were tested in three cases: first, with no field; second, with a field of 680 Gs at 40 Hz; and third, with a field of 680 Gs at 300 Hz. No effects of the field frequency were observed on DK/δ. A slight increase of DK/δ (within the experimental error) was observed for all the salts when the field was applied.

The three cases of the electromagnetic field were also applied to tests with pure water, and no effect of the field on pure water permeability was detected. However, the pure water permeability increased in the first 85 hours of the tests. To identify whether the increase in the pure water permeability was an effect of the electromagnetic field or due to the fact that the membrane did not reach an equilibrium in the first 85 hours, additional tests were performed with $CaCl_2$ at 0.1 M.

The tests with $CaCl_2$ at 0.1 M constituted the last phase of the project. Six tests with $CaCl_2$ at 0.1 M were performed for a total duration of 408 hours. The first three tests were performed with no field, and the next three tests were performed with a field of 680 Gs at 40 Hz. The pure water permeation was measured after each salt test, and its values increased continuously for the duration of 408 hours. The decrease in the normalized product flow as well as the increase in the product concentration suggested that the membrane had reached the equilibrium and it was functioning in the normal regime. Therefore, the continuous increase in A is believed to be an effect of the electromagnetic field. The salt permeability, DK/δ, increased from test 1 to test 3 when no field was applied and decreased from test 4 to test 6 when the field was on. The averages of DK/δ with and without field differed by approximately 7%.

The results from the last phase with the new RO system has shown that, due to the electromagnetic field, the salt permeability decreases, although by a small extent. The increase of the pure water permeability after the electromagnetic field was applied to salt solution tests suggest that possible modifications in the membrane materials may occur due to the electromagnetic field.

6. Recommendations

The effect of the electromagnetic field could be better observed if two membranes were studied in parallel in the same system. One membrane is for control and should have no field applied. The second membrane has an electromagnetic field applied on a continuous basis. The system parameters should be the same for both membranes (feed concentration and temperature, and operating pressure). The scaling potential should be enhanced by using solutions of $CaCO_3$ as feed. It was important to have the system operating on a continuous basis for several months to observe the long-term effects, in order to simulate the real conditions of operating RO desalination systems.

The construction of the solenoid right on the pressure vessel must be avoided. An air gap was required for ventilation or for placement of a cooling system. A better overall temperature control can be assured if the solenoid is constructed of special wire with an integrated cooling system. This will not only assure a constant product temperature but also a prolonged functioning of the solenoid at high currents.

7. Appendix

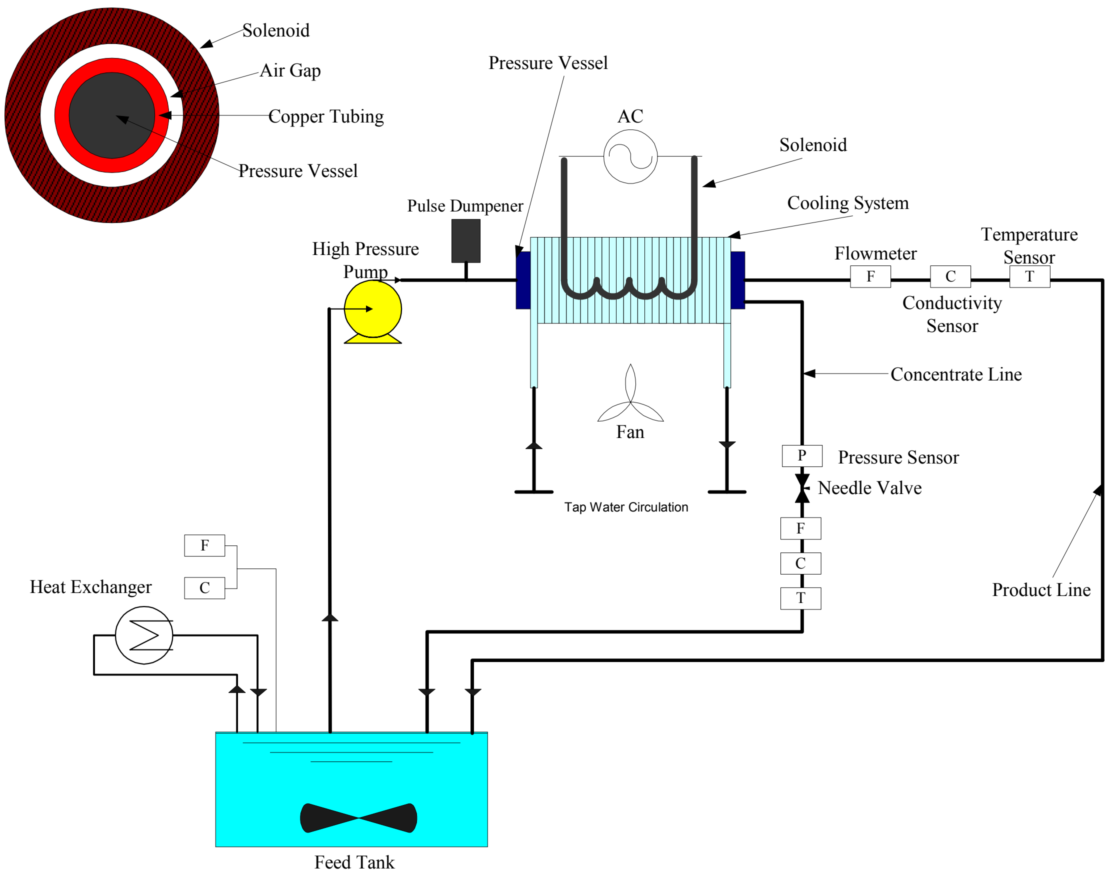

Figure A.1 Schematic diagram of the modified RO system.

Table A.1. **Components of the modified system and their characteristics**

Part	Manufacturer	Characteristics
RO System		
High Pressure Pump+Motor	Hydra-Cell	2 gal/min
		up to 1,000 psi
Pulse Dampener	Blacoh Fluid Control	Stainless Steel, up to 1,500 psi
Pressure Vessel	Crane Environmental	2.5"x14"
		Fiberglass
		max 1,000 psi
RO Membrane	Filmtec	100 gpd
		R = 99.2
Clamping System	USF Shop	Aluminum
Pressure Gauge	Amazon Hose	0-1,000psi
Needle Valve	Swagelok	Stainless Steel
High Pressure Tubing	Amazon Hose	L = 3'
Reinforced Tubing	Home Depot	L=20', D=3/4"
Cooling System		
Cupper Tubing	Home Depot	L =10'
		D =1/8"
Fan	Home Depot	3 speeds
Electromagnetic System		
Solenoid	Tampa Bay Armature	800 turns
		7 layers
		f 0.105

Figure A.2. Assembly of the pressure vessel, solenoid and the support system for the modified RO system.